New isotope ^{44}Si and systematics of the production cross sections of the most neutron-rich nuclei

O. B. Tarasov,[1,2,*] T. Baumann,[1] A. M. Amthor,[1,3] D. Bazin,[1] C. M. Folden III,[1] A. Gade,[1,3] T. N. Ginter,[1] M. Hausmann,[1] M. Matos,[1] D. J. Morrissey,[1,4] A. Nettleton,[1,3] M. Portillo,[1] A. Schiller,[1] B. M. Sherrill,[1,3] A. Stolz,[1] and M. Thoennessen[1,3]

[1]*National Superconducting Cyclotron Laboratory, Michigan State University, East Lansing, Michigan 48824, USA*

[2]*Flerov Laboratory of Nuclear Reactions, JINR, RU-141980 Dubna, Moscow region, Russian Federation*

[3]*Department of Physics and Astronomy, Michigan State University, East Lansing, Michigan 48824, USA*

[4]*Department of Chemistry, Michigan State University, East Lansing, Michigan 48824, USA*

(Received 30 March 2007; published 25 June 2007)

The results of measurements of the production of neutron-rich nuclei by the fragmentation of a ^{48}Ca beam at 142 MeV/nucleon are presented. Evidence was found for the production of a new isotope that is the most neutron-rich silicon nuclide, ^{44}Si, in a net neutron pickup process. A simple systematic framework was found to describe the production cross sections based on thermal evaporation from excited prefragments that allows extrapolation to other weak reaction products.

DOI: 10.1103/PhysRevC.75.064613 PACS number(s): 27.40.+z, 25.70.Mn

I. INTRODUCTION

The study of properties of the most exotic isotopes continues to be one of the important tasks in experimental nuclear physics. In addition, masses, lifetimes, and properties of excited states are important not only for models of nuclear structure but also for the understanding of astrophysical processes. The first step in the study of a new exotic nucleus is its observation, which for neutron-rich nuclei demonstrates its stability with respect to particle emission.

The neutron dripline is only confirmed up to $Z = 8$ ($^{24}O_{16}$) by work at projectile fragmentation facilities in the U.S. [1], France [2,3], and Japan [4]. As indicated in Fig. 1, the dripline rapidly shifts to higher neutron numbers at $Z = 9$ and $^{31}F_{22}$ has been observed by several groups [5–7]. This shift makes the search for the neutron dripline in this region especially difficult but none the less important. Experiments at RIKEN in Japan [5] and at GANIL in France [6] observed the two heaviest isotopes along the $A = 3Z + 4$ line, $^{34}Ne_{24}$ and $^{37}Na_{26}$, by the fragmentation of $^{48}Ca_{28}$ projectiles. The heavier nuclei in this series, $^{40}Mg_{28}$ and $^{43}Al_{30}$, are unobserved at present. All nuclei with $A = 3Z + 3$ up to $Z = 12$ have been shown to be unbound. The neighboring nuclei with $A = 3Z + 2$ have been observed up to $^{41}Al_{28}$ but the production of the heavier nuclei from a ^{48}Ca beam requires a reaction with a net neutron pickup.

In the present work a series of measurements was carried out to search for new neutron-rich isotopes in this region and to measure the cross sections for production of these isotopes. A particular candidate for study is $^{44}Si_{30}$, a nuclide that has two more neutrons than the projectile nucleus. Nucleon pickup products have been observed among fragmentation products, see for example Refs. [8–10], but their cross sections are significantly lower than those of pure fragmentation processes. The new data for the production cross sections builds upon the recent results from Mocko *et al.* [10] and can provide a path to the production of the most neutron-rich nuclei.

II. EXPERIMENTAL DETAILS

A 142 MeV/u ^{48}Ca beam from the coupled cyclotron facility at the National Superconducting Cyclotron Laboratory was used to irradiate either a ^{9}Be target (724 mg/cm^2) or a $^{\text{nat}}$W target (1111 mg/cm^2) located at the normal target position of the A1900 fragment separator [11]. The tungsten target was used due to its high melting point even though it is not monoisotopic. The average primary beam intensity for the measurements of the most exotic fragments was 70 pnA. The momentum acceptance of the separator was either $\Delta p/p = \pm 1\%$ or $\pm 2\%$ and the angular acceptance was 8 msr. The experimental setup and analysis procedures used for this experiment were similar to those described in Refs. [7,10,12,13] and only the differences will be briefly described. The time of flight of each particle that reached the focal plane was measured in two ways: first, over the 17.8 m flight path between a plastic scintillator (22 mg/cm^2 thick) located at the second dispersive image (image 2) and a 10 cm thick plastic backstop scintillator located at the focal plane of the separator, and also over the entire 35.6 m flight path of the A1900 fragment separator by measuring the arrival time relative to the phase of the cyclotron rf-signal. The magnetic rigidity for each particle was determined by the separator setting plus a correction based on the position measurements at image 2 with the plastic scintillator, and at the focal plane of the separator using a set of parallel-plate avalanche counters (PPACs). The standard focal plane detector setup was augmented to have three silicon PIN diodes (50×50 mm^2 by 496 μm, 528 μm, and 526 μm thick) to enable multiple measurements of the energy-loss of the fragments and thus provide redundant determinations of the nuclear charge of each fragment. The simultaneous measurements of multiple ΔE signals, the magnetic rigidity, a scintillator signal proportional to the total energy, as well as the flight times for each particle provided an unambiguous identification of the atomic number, charge state, and mass of the produced fragments. The position and angle measurements with PPACs at the focal plane also enabled discrimination against various scattered particles.

The relative beam current was monitored continuously by a small BaF_2 crystal mounted on a photomultiplier tube near

*tarasov@nscl.msu.edu

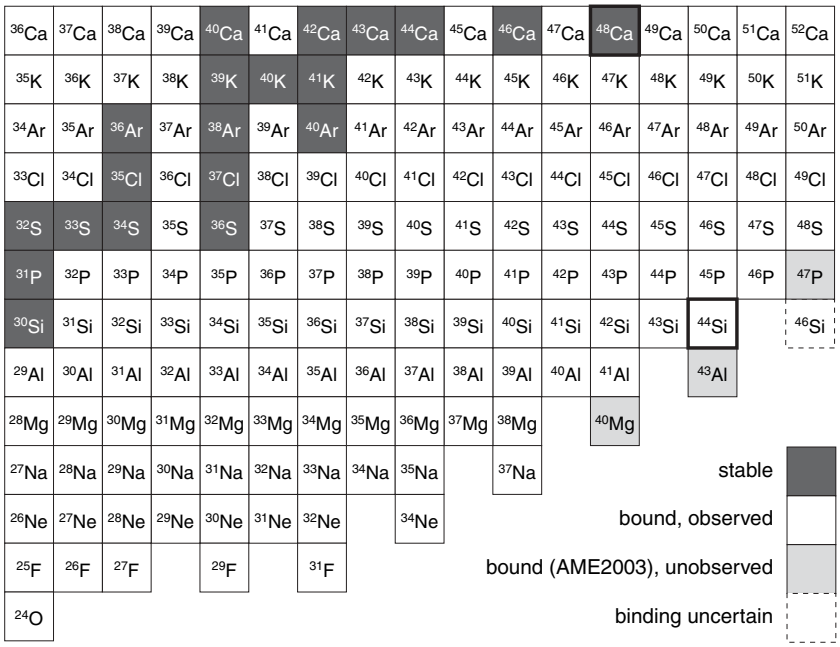

FIG. 1. The region of the chart of nuclides under investigation in this work.

the target position that provided a normalization for the data obtained at different magnetic rigidities. In order to map out the momentum distributions of the fragmentation products and provide the production yields, the magnetic rigidity of the separator was varied stepwise from 4.13 Tm to 4.89 Tm. The momentum distributions of isotopes between magnesium and phosphorus that were present at these settings were analyzed during the experiment. These measured distributions are in good agreement with LISE++ [14] calculations, using either the universial parametrization [15] or the model by Morrissey [16], so that the optimum separator setting for the heaviest isotopes (that were produced at a higher rigidity setting with very low rates) could be inferred from our LISE++ calculations. Once the optimum setting was determined, an achromatic energy-loss degrader (^{27}Al, 151 mg/cm^2) was inserted at image 2 of the A1900 separator in addition to the plastic scintillator to cut down the range of atomic numbers of the fragments reaching the focal plane.

A search for ^{44}Si was carried out by performing several runs totaling 4.3 h with the tungsten target and 5.8 hours with the beryllium target at a setting optimized for ^{38}Mg and ^{41}Al at a rigidity of 5.045 Tm (4.9598 Tm after image 2). The combination of the higher energy loss of silicon isotopes in the thick targets and the image 2 degrader plus the expected momentum downshift due to nucleon pickup (cf. [9]) placed ^{44}Si in the acceptance of the fragment separator. Three events identified as ^{44}Si nuclei were observed during the measurements with the tungsten target (see Fig. 2) and none were observed with the beryllium target. The overall efficiency of the system was found to be 73^{+19}_{-15}% and 39^{+19}_{-12}% when running with the tungsten and beryllium targets, respectively. The efficiency was dominated by the deadtime of the data acquisition system and the discrimination against pileup events in the focal plane detector. Trigger rates averaged 200 Hz for the runs with the tungsten target, and 450 Hz with the beryllium target. The simulated angular transmission ranged from 77% for ^{38}Mg to 84% for ^{44}Si with an estimated uncertainty of 5% using the technique described by Mocko *et al.* [10].

III. RESULTS AND DISCUSSION

The cross sections for the production of neutron-rich silicon isotopes from this work are shown in Fig. 3 and given in Table I along with the cross sections recently reported by Mocko *et al.* [10] for the reaction of ^{48}Ca with ^{9}Be and ^{181}Ta at the same bombarding energy. For the purpose of comparison we will consider the tantalum and tungsten targets as equivalent. The cross sections for reaction with the tungsten

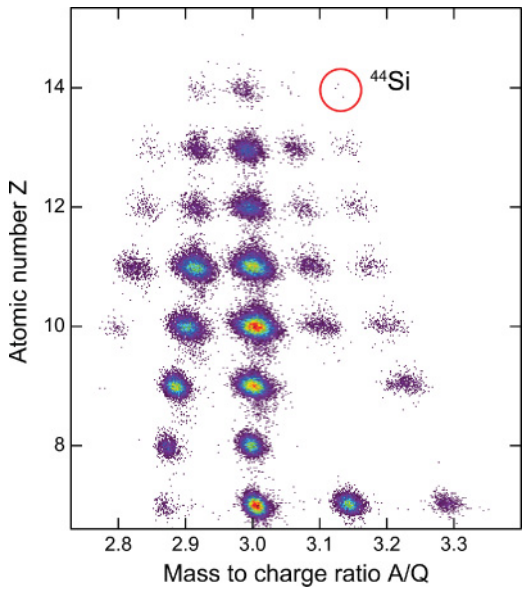

FIG. 2. (Color online) Particle identification plot of atomic number Z versus mass-to-charge ratio A/Q for $Z = 7$ to 15.

TABLE I. Cross sections for neutron-rich Mg and Si isotopes observed in this work.

Isotope	σ (W target) (mb)	σ (Be target) (mb)
^{36}Mg	$(5 \pm 1) \times 10^{-6}$	$(6^{+4}_{-3}) \times 10^{-7}$
^{37}Mg	$(9^{+3}_{-2}) \times 10^{-8}$	$(1.6^{+0.8}_{-0.7}) \times 10^{-8}$
^{38}Mg	$(4 \pm 1) \times 10^{-8}$	$(4 \pm 1) \times 10^{-9}$
^{41}Si	$(1.3^{+0.6}_{-0.8}) \times 10^{-5}$	
^{42}Si	$(9 \pm 3) \times 10^{-7}$	$(9^{+7}_{-6}) \times 10^{-8}$
^{43}Si	$(5 \pm 2) \times 10^{-9}$	$(9^{+5}_{-4}) \times 10^{-10}$
^{44}Si	$(7 \pm 5) \times 10^{-10}$	

target are larger than those with beryllium by factors that range from approximately 2.5 at $A = 38$ to about 9 at $A = 42$, values that become significantly larger than the ratio of the geometric reaction cross sections σ_r

$$\frac{\sigma_r(\mathrm{W})}{\sigma_r(\mathrm{Be})} \sim \frac{(A^{1/3}(\mathrm{Ca}) + A^{1/3}(\mathrm{W}))^2}{(A^{1/3}(\mathrm{Ca}) + A^{1/3}(\mathrm{Be}))^2} = 2.7.$$

The data show a smooth decline with increasing mass number (or neutron number) up to $A = 42$, and then a precipitous drop by about a factor of 110 for the two silicon isotopes with more neutrons than the projectile. The slope of the data compares well to the EPAX 2.15 systematics [17] although the data sets lie below the predictions. The EPAX parametrization describes the products of *limiting fragmentation* that occurs at high bombarding energies and only depends on the sizes of the target and projectile. Closer comparison of the prediction to the data shows that the cross sections for ^{42}Si from both targets are more suppressed than the average of the lighter isotopes. This is consistent with the idea that the most neutron-rich nuclei come from the decay of excited primary fragments that are themselves even more neutron-rich (and suppressed by the process of significant neutron transfer from the target at these bombarding energies due to momentum mismatch).

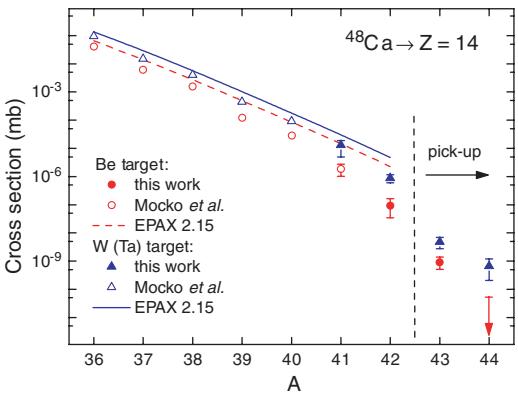

FIG. 3. (Color online) The cross sections for production of neutron-rich silicon nuclei from Ref. [10] and the present work. The data with $A < 43$ (i.e., $N < 28$) are compared to the EPAX systematics for limiting fragmentation [17].

Models of nuclear reactions used for counting rate estimates, like the intranuclear-cascade plus evaporation model [18] or abrasion-ablation in LISE++ [19] cannot reproduce the low yields of the exotic nuclei observed in this study. Thus it is not possible to make reliable predictions for further work. As a starting point, the cross sections in peripheral two-body reactions have been analyzed in the framework of the Q_{gg} systematics for a long time [20]. The central idea of the Q_{gg} systematics is that the products are created in a statistical, thermal process and the cross section should follow the expression

$$\sigma(Z, A) = f(Z) \exp(Q_{gg}/T) \quad \text{or} \quad \ln(\sigma(Z, A)) \propto Q_{gg},$$

where Q_{gg} is the simple difference between the mass excesses of the ground states of the product and reactant nuclei and T is an effective temperature that is fitted to the data. Such an ansatz is reasonable at low energies when the nuclei undergo a slow transfer process and for the observation of projectile residues from mass-asymmetric reactions where the bulk of the excitation energy is carried by the heavy partner. Over the years a number of measurements of light products at higher energies have found some agreement with this model as can be seen in Fig. 4 (left panels) for the data from this study combined with the data from Mocko *et al.* [10]. The data for the most neutron-rich isotopes in each chain tend toward straight lines but the bulk of the data with the highest yields, highest precision, and lowest Q-values behaves very differently. It is important to realize that Q_{gg} is most sensitive to the mass of the lighter fragment since the binding energy changes most rapidly with neutron and proton number in the low mass region. Previous studies that were used to develop the Q_{gg} systematics relied on the analysis of the distributions of the light fragment from reactions in normal kinematics [20]. In the present work the lighter fragment is the *target residue* in the case of the beryllium target, whereas it is the *projectile residue* in the case of the tungsten target. The dominant factor in the exponential is then either the unobserved fragment [beryllium target, panel (b) of Fig. 4] or the observed fragment [heavy target, panel (a) of Fig. 4].

Projectile fragmentation is usually not described as a two-body process, but rather as a sudden process that forms an excited prefragment followed by statistical decay. Charity [23] has pointed out that the sequential evaporation of light particles from sufficiently excited nuclei follows a general pattern that leads to a somewhat uniform distribution of final products. This uniform distribution underlies the EPAX systematics. In the usual case neutrons are emitted preferentially from excited nuclei until the point at which the ratio of the widths for statistical emission of neutrons to charged particles, Γ_N/Γ_Z, becomes small. Note that this expression includes neutrons and protons bound in clusters as described in Ref. [23]. The individual emission widths, Γ_N and Γ_Z, contain a number of factors but most of these factors approximately cancel in the ratio and the largest remaining term is an exponential of the difference between the neutron and proton separation energies, S_n and S_p:

$$\Gamma_N/\Gamma_Z \propto \exp(S_p - S_n). \quad (1)$$

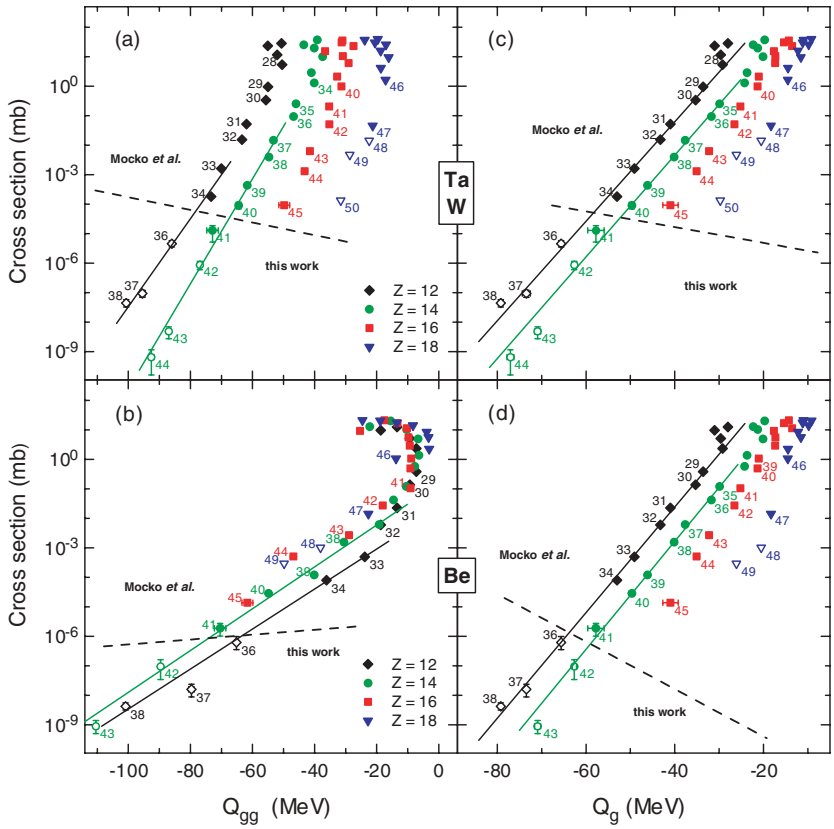

FIG. 4. (Color online) The variation of the cross sections for the production of neutron rich nuclei as a function of the two-body Q values [Q_{gg}, left panels (a), (b)] and as a function of the one-body Q value [Q_g, right panels (c), (d)], see text for details. Upper panels (a), (c) show data for W (Ta), lower panels (b), (d) for Be targets. Each symbol is labeled with the respective mass number. Data from the present work (below the dashed lines in each panel) were combined with data from Ref. [10]. Solid symbols represent Q-value calculations based on the measured mass values, and open symbols based on the recommended values [21,22]. The lines represent exponential fits of the most neutron-rich isotopes for each chain.

The separation energies contain the masses of the daughter isotopes, thus, we can expect an exponential dependence of the yield on the mass difference between the daughter nuclei for proton and neutron emission in this model. The masses are not known experimentally for most of the very neutron-rich nuclei in this study. In an attempt to extract the average systematic behavior the cross sections are plotted as a function of

$$Q_g = ME(Z = 20, A = 48) - ME(Z, A) \qquad (2)$$

in Fig. 4 (right panels), where $ME(Z, A)$ is the mass excess in MeV. Q_g is a function that compares the relative binding energies of all of the projectile fragments without regard to the target nucleus and is a plausible basis for comparison of products from a process that creates a small set of highly excited nuclei that then statistically populate all of the available mass surface. The figure shows that this function provides an excellent systematization of the data with each isotopic chain falling on a straight line. Moreover, the slopes or inverse temperatures decrease with atomic number and go from about 1.2 (Ar from Be) to a maximum of $T \approx 2.5$ MeV (Mg and Si from Be and Ta). The line from the production of magnesium isotopes can be extrapolated to predict a cross section of 0.04 ± 0.01 pb for ^{40}Mg, as yet unobserved.

IV. SUMMARY

The study of the production of the most neutron-rich silicon isotopes provided evidence for the existence of a new isotope, ^{44}Si, in a high energy reaction that requires the net transfer of two neutrons to the projectile. The decline of the cross sections for the production of silicon isotopes with increasing mass number was found to parallel the EPAX parametrization but at a lower level, up to the point that neutron pickup intermediates begin to be important. The measured cross sections for nuclei with more neutrons than the projectile fall by approximately two orders of magnitude below a logarithmic extrapolation from the lighter isotopes.

The variation of the cross sections for a large range of reaction products were considered in the framework of the well-known Q_{gg} systematics developed for low-energy two-body reactions. Only the tails of the distributions had the expected linear dependence and the applicability of this model to projectile residues from reverse kinematical reactions is entirely questionable. On the other hand, all of the available data were shown to follow a very smooth systematic dependence, independent of the target, with the mass of the observed fragment. An extrapolation of the data using the new one-body Q_g systematics indicates that a search for ^{40}Mg is feasible.

ACKNOWLEDGMENTS

The authors would like to acknowledge the work of the operations staff of the NSCL to develop the intense ^{48}Ca beam necessary for this study. This work was supported by the U.S. National Science Foundation under grant PHY-06-06007. One of the authors (M.M.) acknowledges support by the U.S. National Science Foundation under grant PHY-02-16783 (Joint Institute of Nuclear Astrophysics).

[1] M. Fauerbach, D. J. Morrissey, W. Benenson, B. A. Brown, M. Hellström, J. H. Kelley, R. A. Kryger, R. Pfaff, C. F. Powell, and B. M. Sherrill, Phys. Rev. C **53**, 647 (1996).
[2] D. Guillemaud-Mueller, J. C. Jacmart, E. Kashy, A. Latimier, A. C. Mueller, F. Pougheon, A. Richard, Yu. E. Penionzhkevich, A. G. Artukh, A. V. Belozyorov *et al*., Phys. Rev. C **41**, 937 (1990).
[3] O. Tarasov, R. Allatt, J. C. Angélique, R. Anne, C. Borcea, Z. Dlouhý, C. Donzaud, S. Grévy, D. Guillemaud-Mueller, M. Lewitowicz *et al*., Phys. Lett. **B409**, 64 (1997).
[4] H. Sakurai, S. M. Lukyanov, M. Notani, N. Aoi, D. Beaumel, N. Fukuda, M. Hirai, E. Ideguchi, N. Imai, M. Ishihara *et al*., Phys. Lett. **B448**, 180 (1999).
[5] M. Notani, H. Sakurai, N. Aoi, Y. Yanagisawa, A. Saito, N. Imai, T. Gomi, M. Miura, S. Michimasa, H. Iwasaki *et al*., Phys. Lett. **B542**, 49 (2002).
[6] S. M. Lukyanov, Yu. E. Penionzhkevich, R. Astabatyan, S. Lobastov, Yu. Sobolev, D. Guillemaud-Mueller, G. Faivre, F. Ibrahim, A. C. Mueller, F. Pougheon *et al*., J. Phys. G **28**, L41 (2002).
[7] E. Kwan, D. J. Morrissey, D. A. Davies, M. Steiner, C. S. Sumithrarachchi, and L. Weissman, AIP Conf. Proc. **884**, 213 (2007).
[8] G. A. Souliotis, D. J. Morrissey, N. A. Orr, B. M. Sherrill, and J. A. Winger, Phys. Rev. C **46**, 1383 (1992).
[9] R. Pfaff, D. J. Morrissey, M. Fauerbach, M. Hellström, J. H. Kelley, R. A. Kryger, B. M. Sherrill, M. Steiner, J. S. Winfield, J. A. Winger *et al*., Phys. Rev. C **51**, 1348 (1995).
[10] M. Mocko, M. B. Tsang, L. Andronenko, M. Andronenko, F. Delaunay, M. Famiano, T. Ginter, V. Henzl, D. Henzlová, H. Hua *et al*., Phys. Rev. C **74**, 054612 (2006).
[11] D. J. Morrissey, B. M. Sherrill, M. Steiner, A. Stolz, and I. Wiedenhöver, Nucl. Instrum. Methods Phys. Res. B **204**, 90 (2003).
[12] T. Baumann, N. Frank, B. A. Luther, D. J. Morrissey, J. P. Seitz, B. M. Sherrill, M. Steiner, J. Stetson, A. Stolz, M. Thoennessen *et al*., Phys. Rev. C **67**, 061303(R) (2003).
[13] A. Stolz, T. Baumann, N. H. Frank, T. N. Ginter, G. W. Hitt, E. Kwan, M. Mocko, W. Peters, A. Schiller, C. S. Sumithrarachchi *et al*., Phys. Lett. **B627**, 32 (2005).
[14] O. B. Tarasov and D. Bazin, Nucl. Phys. **A746**, 411 (2004).
[15] O. Tarasov, Nucl. Phys. **A734**, 536 (2004).
[16] D. J. Morrissey, Phys. Rev. C **39**, 460 (1989).
[17] K. Sümmerer and B. Blank, Phys. Rev. C **61**, 034607 (2000).
[18] D. J. Morrissey, L. F. Oliveira, J. O. Rasmussen, G. T. Seaborg, Y. Yariv, and Z. Fraenkel, Phys. Rev. Lett. **43**, 1139 (1979).
[19] O. B. Tarasov and D. Bazin, Nucl. Instrum. Methods Phys. Res. B **204**, 174 (2003).
[20] C. K. Gelbke, C. Olmer, M. Buenerd, D. L. Hendrie, J. Mahoney, M. C. Mermaz, and D. K. Scott, Phys. Rep. **42**, 311 (1978).
[21] G. Audi, A. H. Wapstra, and C. Thibault, Nucl. Phys. **A729**, 337 (2003).
[22] O. B. Tarasov and D. Bazin, Tech. Rep. MSUCL1248, NSCL, Michigan State University (2002).
[23] R. J. Charity, Phys. Rev. C **58**, 1073 (1998).